Acta Crystallographica Section F
**Structural Biology and Crystallization Communications**
ISSN 1744-3091

# Crystallization and preliminary X-ray diffraction analysis of the dimerization domain of the tumour suppressor ING4

**Simone Culurgioni,[a] Inés G. Muñoz,[b] Alicia Palacios,[a] Pilar Redondo,[b] Francisco J. Blanco[a,c]* and Guillermo Montoya[b]***

[a]Structural Biology Unit, CIC bioGUNE, Parque Tecnológico de Bizkaia, Edificio 800, 48160 Derio, Spain, [b]Macromolecular Crystallography Group, Structural Biology and Biocomputing Programme, Spanish National Cancer Centre (CNIO), Melchor Fernández Almagro 3, 28029 Madrid, Spain, and [c]IKERBASQUE, Basque Foundation for Science, 48011 Bilbao, Spain

Correspondence e-mail: fblanco@cicbiogune.es, gmontoya@cnio.es

Received 3 February 2010
Accepted 17 March 2010

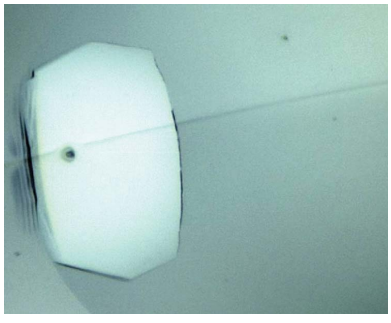



Inhibitor of growth protein 4 (ING4) belongs to the ING family of tumour suppressors and is involved in chromatin remodelling, in growth arrest and, in cooperation with p53, in senescence and apoptosis. Whereas the structure and histone H3-binding properties of the C-terminal PHD domains of the ING proteins are known, no structural information is available for the N-terminal domains. This domain contains a putative oligomerization site rich in helical structure in the ING2–5 members of the family. The N-terminal domain of ING4 was overexpressed in *Escherichia coli* and purified to homogeneity. Crystallization experiments yielded crystals that were suitable for high-resolution X-ray diffraction analysis. The crystals belonged to the orthorhombic space group *C*222, with unit-cell parameters $a = 129.7$, $b = 188.3$, $c = 62.7$ Å. The self-rotation function and the Matthews coefficient suggested the presence of three protein dimers per asymmetric unit. The crystals diffracted to a resolution of 2.3 Å using synchrotron radiation at the Swiss Light Source (SLS) and the European Synchrotron Radiation Facility (ESRF).

## 1. Introduction

The ING genes have been identified and characterized as type II tumour-suppressor genes (TSGs). The proteins encoded by these genes are involved in numerous signalling mechanisms and especially in two tumour-suppressor pathways: apoptosis and senescence. The ING proteins contain a flexible and nonconserved central region containing the nuclear localization sequence (NLS) and a conserved plant homeodomain (PHD) finger at their C-termini which is responsible for histone H3 tail recognition (Bienz, 2006; Mellor, 2006). The N-terminal regions of these proteins are more variable, but contain a leucine zipper-like (LZL) region and a novel conserved region (NCR) (Ythier *et al.*, 2008). The LZL region is present in all members of the family except ING1. This region has been proposed to be responsible for homo- or hetero-oligomerization between the members of the family (He *et al.*, 2005).

Studies in yeast have shown that ING proteins are components of the histone acetyl transferase (HAT) and histone deacetylase (HDAC) complexes (Loewith *et al.*, 2000; Soliman & Riabowol, 2007). In fact, in human cells each ING protein associates with different HAT or HDAC complexes. For example, ING1 and ING2 associate with the mSin3a HDAC1/2 complex, ING3 with the Tip60/NuA4 complex, ING4 with the HBO1 complex and ING5 with the HBO1 and the MOZ/MORF complexes (Doyon *et al.*, 2006). Moreover, ING4 is strictly required for HBO1 to acetylate histone H4 (Doyon *et al.*, 2006), histone H2A (Iizuka *et al.*, 2008) and histone H3 (Hung *et al.*, 2009). Recent studies have suggested that ING4 mediates crosstalk between the trimethylation of histone H3 at lysine 4 (H3K4me3) and the acetylation of histone H3. The C-terminal PHD domain specifically recognizes H3K4me3 tails (Palacios *et al.*, 2006, 2008), while the N-terminal domain of ING4 has been suggested to associate with the HBO1 acetylase complex (Hung *et al.*, 2009). We have recently found that ING4 forms homodimers in solution through its N-terminal domain (Palacios *et al.*, 2010). Here, we report the crystallization of this domain of ING4, which is essential for the elucidation of its structure.

## 2. Materials and methods

### 2.1. Gene, plasmids and primers

The ING4 (UniProt code Q9UNL4) DNA sequence used was optimized for *Escherichia coli* expression according to the preferential codon usage (Palacios *et al.*, 2010). ING4 N-terminal constructs were obtained from the ING4(1–118) clone (Palacios *et al.*, 2010), inserting a stop codon by site-directed mutagenesis, using the primers GCCTGGATACCGATTAGGCTCGTTTCGAAG and CTTCGAAACGAGCCTAATCGGTATCCAGGC for ING4(1–103), GATACCGATCTGGCTTGATTCGAAGCGGATCTG and CAGATCCGCTTCGAATCAAGCCAGATCGGTATC for ING4(1–105), GGCTCGTTTCGAATAGGATCTGAAAGAG and CTCTTTCAGATCCTATTCGAAACGAGCC for ING4(1–109).

### 2.2. Protein expression and purification

*E. coli* BL21 (DE3) cells were transformed with the plasmid pET11d(+) containing the ORF coding for the N-terminal sequence of ING4 (residues 1–103, 1–105, 1–109 and 1–118). The N-terminal domain of ING4 (N-term) was overexpressed in LB medium at 310 K. The culture was induced for 3 h after addition of 0.5 m*M* IPTG when the $OD_{600}$ was ∼0.6–0.8. Selenomethionine-labelled N-term ING4 was expressed using the same strain. The bacterial pellet was resuspended in 100 m*M* Tris–HCl pH 8.0 containing protease inhibitors (Complete EDTA-free tablets, Roche) and the cells were disrupted by sonication. The lysate was cleared by centrifugation (20 000*g* for 1 h). The supernatant was applied onto a 5 ml HiTrap Q Sepharose XL column (GE Healthcare) and the protein was eluted using an NaCl gradient (0–1 *M*). The fractions containing N-term ING4 were pooled, concentrated and diluted five times in 100 m*M* Tris–HCl pH 8.0 to lower the NaCl concentration. The sample was then loaded onto a 5 ml Mono Q 5/50 GL column (GE Healthcare)

**Table 1**
Initial crystallization conditions of the ING4 dimerization domain.

| Protein construct | Commercial crystallization screen | Condition Nos. |
|---|---|---|
| ING4(1–109) | JBScreen Kinase 3 | 18, 23 |
| | JCSG+ Suite | 43 |
| | Precipitant Synergy Primary | 29, 36, 55, 64 |
| | Precipitant Synergy Expanded 67% | 29, 59 |
| ING4(1–105) | JBScreen Kinase 1 | 8, 9, 20 |
| | JBScreen Kinase 2 | 3 |
| | JBScreen Kinase 3 | 8, 11, 14, 20, 23 |
| | JCSG+ Suite | 49 |
| | EasyXtal PACT Suite | 22, 23, 89, 96 |
| | Precipitant Synergy Primary | 35, 53 |
| | Crystal Screen Cryo | 22, 38 |

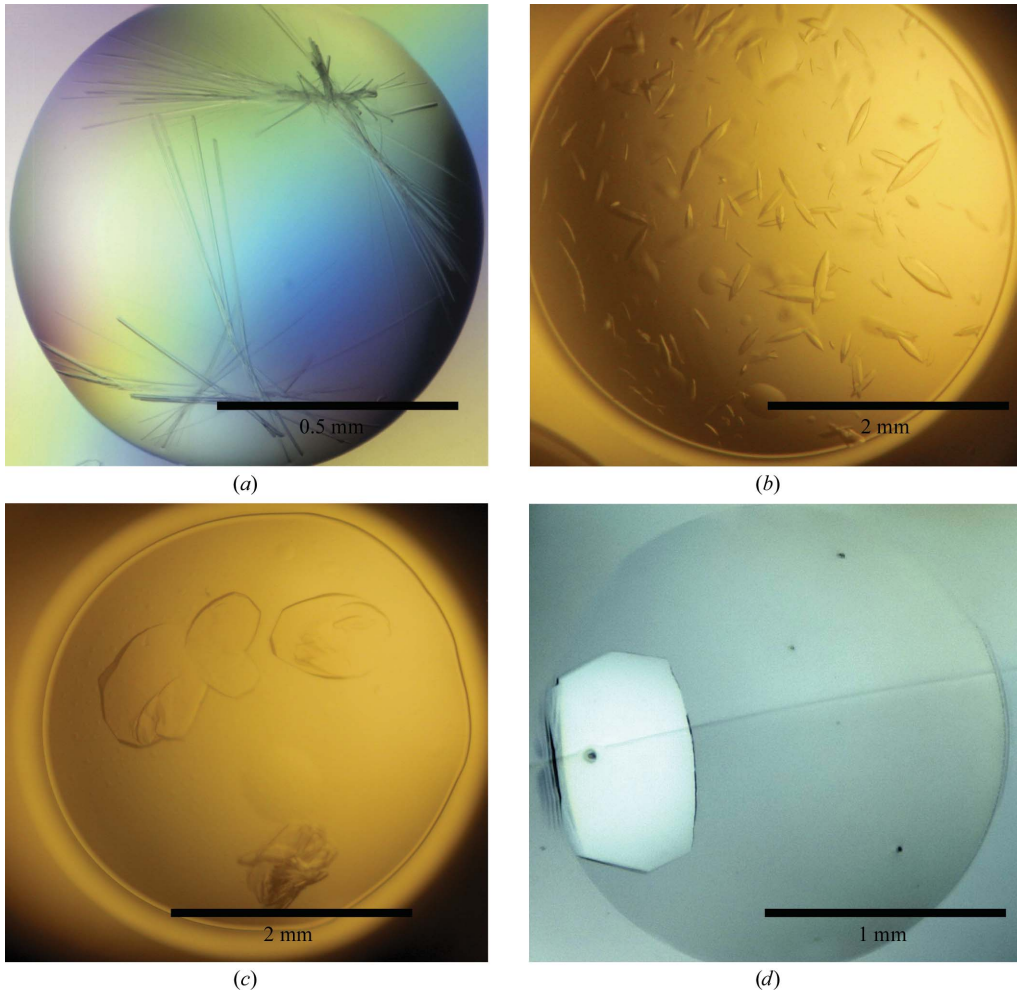


(*a*) (*b*) (*c*) (*d*)

**Figure 1**
ING4(1–105) crystal optimization: (*a*) starting hits, (*b*) crystals after optimization of pH and PEG 3350 concentration, (*c*) crystals optimized with Optisalt solution and (*d*) final crystals obtained using Silver Bullet condition No. A3. The crystals are generally large plates with hexagonal shape and occasionally measured up to 2 mm in their longest dimension.

**Table 2**
Data-collection statistics for the ING4 dimerization-domain crystals.

Values in parentheses are for the outermost resolution shell.

| | |
|---|---|
| No. of crystals | 1 |
| Beamline | ID23-1 |
| Wavelength (Å) | 0.979 |
| Detector | ADSC Quantum Q315r |
| Crystal-to-detector distance (mm) | 367.78 |
| Rotation range per image (°) | 0.5 |
| Total rotation range (°) | 0–180 |
| Exposure time per image (s) | 1.5 |
| Resolution range (Å) | 47.09–2.27 (2.27–2.40) |
| Space group | *C*222 |
| Unit-cell parameters (Å, °) | $a$ = 129.7, $b$ = 188.3, $c$ = 62.7 |
| Mosaicity (°) | 0.183 |
| Total No. of measured intensities | 234424 |
| Unique reflections | 34723 |
| Multiplicity | 6.8 (3.3) |
| Mean $I/\sigma(I)$ | 11.1 (2.1) |
| Completeness (%) | 96.8 (96.8) |
| $R_{\rm merge}$(%) | 9.3 (35.7) |
| $R_{\rm meas}$ or $R_{\rm r.i.m.}$† (%) | 4.4 (24.1) |
| $R_{\rm anom}$ (%) | 5.7 (28.0) |
| Overall $B$ factor from Wilson plot (Å$^2$) | 44.460 |

† As described in Weiss (2001) and Evans (2006).

previously equilibrated with 100 m*M* Tris pH 8.0. Sample elution was performed by applying a continuous gradient from 0 to 1 *M* NaCl. The purified protein was then concentrated using an Amicon Ultra-system equipped with a 10 kDa cutoff filter and was loaded onto a HiLoad Superdex 75 26/60 column (GE Healthcare) pre-equilibrated with 20 m*M* Tris–HCl pH 8.0 and 300 m*M* NaCl. The fractions containing the protein were pooled, concentrated to 20 mg ml$^{-1}$, flash-frozen in liquid nitrogen and stored at 193 K. The protein concentration was determined from the absorbance at 280 nm using $\varepsilon$ = 7450 $M^{-1}$ cm$^{-1}$. The purity of the sample was checked by Coomassie-stained SDS–PAGE and its polydispersity was evaluated using dynamic light scattering. Finally, complete incorporation of selenomethionine was confirmed by mass spectrometry (data not shown).

### 2.3. ING4 N-terminal domain limited proteolysis assay

After unsuccessful crystallization tests using the ING4 N-terminal construct 1–118 (Palacios *et al.*, 2010), limited proteolysis experiments allowed us to identify a shorter polypeptide construct as an alternative choice for crystallization. The ING4(1–118) fragment was expressed and purified as described previously (Palacios *et al.*, 2010) and diluted to 0.5 mg ml$^{-1}$ in proteolysis buffer (20 m*M* HEPES pH 7.5, 50 m*M* NaCl). Four different experiments were performed in parallel with subtilisin, trypsin, Glu-C and elastase to identify stable proteolytic fragments. Each of the proteases was added to the protein solution in different assays and then incubated at 277 K for 0, 30, 60 and 90 min. Several aliquots were collected from the reaction mixture at the different time periods; the proteolysis reaction was stopped by the addition of SDS–PAGE loading buffer and the samples were stored until they were ready for SDS–PAGE analysis. Proteolysis with GluC and elastase yielded clear discrete bands. These bands were identified by peptide mass-fingerprinting mass spectrometry and N-terminal sequencing.

### 2.4. Crystallization

Crystallization screenings were performed with a Cartesian MicroSys robot (Genomic Solutions) using the sitting-drop method in 96-well MRC plates (Molecular Dimensions) with nanodrops consisting of 0.1 µl protein solution at 20 mg ml$^{-1}$ plus 0.1 µl reservoir solution and a reservoir volume of 60 µl. The initial screens tested were Crystal Screens I, II, Cryo and Lite (Hampton Research), Wizard I and II, Precipitant Synergy Primary, Expanded 67% and Expanded 33% (Emerald BioSystems), EasyXtal PACT Suite and JCSG+ Suite (Qiagen) and JBScreen Kinase 1/2/3/4 (Jena Bioscience). Crystals were obtained under several conditions in nanodrops (Table 1). However, it was not possible to reproduce many of the initial hits in 2 µl drops. The selected crystallization conditions (JBScreen Kinase 3 No. 18, Precipitant Synergy Primary No. 36, Precipitant Synergy Expanded 67% No. 29 and EasyXtal PACT Suite No. 89) were selected based on their producing the best ordered, least clustered, largest and most reproducible crystals. These crystals were tested in-house using an FR591 Bruker generator equipped with Osmic mirrors and a MAR345dtb detector. They generally depicted no or low-resolution diffraction (>20 Å). The condition that was finally selected for crystal optimization was condition No. 89 of EasyXtal PACT Suite [20%(*w*/*v*) PEG 3350, 100 m*M* bis-tris propane pH 8.5, 200 m*M* sodium nitrate; Fig. 1*a*]. These crystals were reproduced in larger sitting drops (1 µl protein solution plus 1 µl mother liquor) and did not diffract. After several cycles of optimization, adjusting the pH and the PEG and salt concentrations, new crystals were obtained that diffracted to 4 Å resolution in-house [24%(*w*/*v*) PEG 3350, 0.1 *M* bis-tris propane pH 7.5, 0.4 *M* sodium nitrate, 10% Optisalt Solution No. 6 (Qiagen); Figs. 1*b* and 1*c*]. The crystal diffraction pattern presented broad spots, indicating a possibly disordered lattice. The final step of optimization consisted of the addition of Silver Bullet solutions (Hampton Research) as additives to this crystallization condition (0.2 µl mother liquor plus 0.4 µl protein solution plus 0.2 µl Silver Bullet). The crystals obtained were tested in-house; the best diffracting condition contained Silver Bullet solution A3 (diglycine/triglycine/tetraglycine/pentaglycine) and yielded hexagonal plate-shaped crystals (∼0.5–2 × 0.5 × 0.05 mm) which diffracted to 2.6 Å resolution and grew in 2–15 d (Fig. 1*d*). The crystals were stuck at the bottom of the sitting drops and were therefore difficult to harvest. This suggested that the plate surface was needed for their nucleation and further growth. To harvest the crystals without damaging them, the crystallization plate was positioned on top of a layer of dry ice for a few seconds, thus inducing shrinkage of the plastic bottom and releasing the crystals into the solution. The crystals were then mounted in cryoloops and cooled in liquid $N_2$ after incubation for a few seconds in mother liquor plus 15% glycerol.

### 2.5. Data collection

As previously mentioned, the crystals were tested in-house using a Bruker FR-591 generator and showed diffraction to 2.6 Å resolution. The rest of the data sets from the ING4 dimerization domain were collected using synchrotron radiation on beamlines ID23-1 at the ESRF and PX at SLS. The diffraction data in Table 2 were recorded using an ADSC-Q315 detector on ID23-1. The best data set was collected using $\Delta\varphi$ = 0.5° and a wavelength of 0.979 Å. Processing and scaling were accomplished with *XDS* (Kabsch, 1988). Statistics of the crystallographic data are summarized in Table 2.

## 3. Results and discussion

The dimerization domain of ING4 (residues 1–118) is an autonomous folding unit as previously observed by CD and NMR (Palacios *et al.*, 2010). This domain did not crystallize after extensive trials; therefore, a limited proteolysis experiment was designed in order to identify stable fragments. Three proteolytic fragments (1–103, 1–105 and 1–

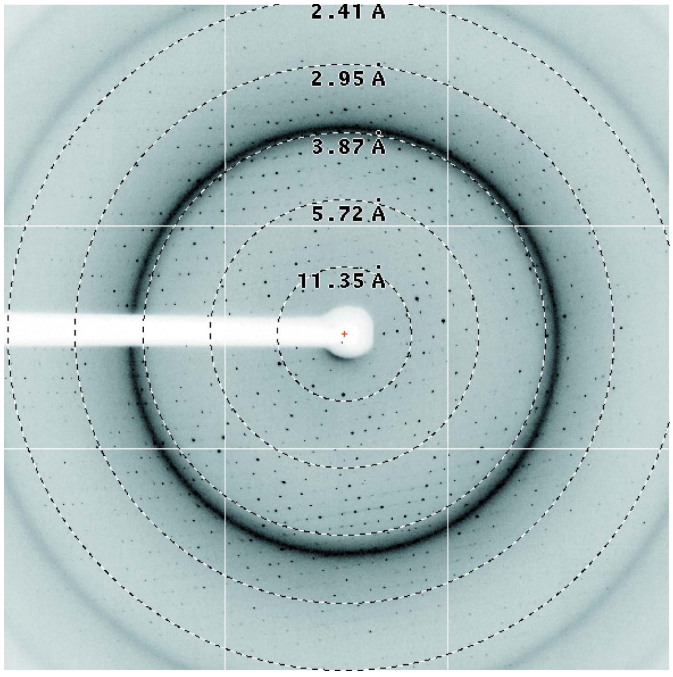


**Figure 2**
Diffraction pattern obtained from the native crystals using synchrotron radiation on the ID23-1 beamline at ESRF, Grenoble.

109) were identified, cloned and purified. Crystallization trials were successful with the 1–105 fragment, which had a theoretical mass of 12 282 Da. However, the purified protein has a measured mass of 12 150 Da, indicating that the initial methionine was processed during expression. The purification procedure yielded around 15 mg pure protein per litre of culture. The recombinant protein was purified using two ion-exchange chromatography columns and a final gel-filtration step. The isolated ING4 dimerization domain was concentrated and used in crystallization assays. The initial hits were clusters of long needle-shaped crystals; several rounds of refinement yielded single ordered plate-like crystals (Fig. 1).

The final optimized crystals were tested using a synchrotron-radiation source to obtain high-resolution data. Several native data sets were collected at 100 K on the PX beamline at SLS, Villigen, while several anomalous dispersion (SAD) data sets were collected at the Se *K* edge on the ID23-1 beamline at ESRF, Grenoble. Using these undulator-equipped beamlines, the crystals diffracted to a maximum resolution of 2.27 Å (at ESRF; Table 2; Fig. 2). The statistics for the data set collected to 2.27 Å resolution on ID23-1 are given in Table 2. The crystals belonged to the orthorhombic space group *C*222, with unit-cell parameters $a = 129.7$, $b = 188.3$, $c = 62.7$ Å. The Matthews coefficient ($V_M = 2.74$ Å$^3$ Da$^{-1}$) and the self-rotation function (data not shown) suggested the presence of six monomers (possibly three dimers) per asymmetric unit and a solvent content of 55%. The collected diffraction data were 96.8% complete, with an overall $I/\sigma(I)$ of 5.9 (see Table 2 for details). The crystals of the selenomethionine-derived protein were used to collect data to solve the structure using single anomalous dispersion at the Se *K* edge. These are the first crystals to be reported for the N-terminal domain of ING4. We believe that the structure of this domain will help in elucidating the molecular mechanism of ING4 oligomerization. These findings could also shed light on the regulation of ING4 activity and on its interaction with the HBO1 acetylase complex, clarifying the role of ING4 in chromatin remodelling. In addition, our data may also provide valuable clues about the behaviour of the N-terminal domains of the other proteins of the ING family.

We would like to thank the staff of the ESRF and SLS biocrystallography beamlines for help with crystallization and data collection. This work was supported by grants from Ministerio de Ciencia e Innovación to FJB (CTQ2008-03115/BQU) and GM (BFU2008-01344), and from the European Union (3D-REPERTOIRE, contract No. LSHG-CT-2005-512028) to FJB and GM. FJB is also grateful for the support from ETORTEK-2008 to CIC bioGUNE.

## References

Bienz, M. (2006). *Trends Biochem. Sci.* **31**, 35–40.
Doyon, Y., Cayrou, C., Ullah, M., Landry, A.-J., Côté, V., Selleck, W., Lane, W. S., Tan, S., Yang, X.-J. & Côté, J. (2006). *Mol. Cell*, **21**, 51–64.
Evans, P. (2006). *Acta Cryst.* D**62**, 72–82.
He, G. H., Helbing, C. C., Wagner, M. J., Sensen, C. W. & Riabowol, K. (2005). *Mol. Biol. Evol.* **22**, 104–116.
Hung, T., Binda, O., Champagne, K. S., Kuo, A. J., Johnson, K., Chang, H. Y., Simon, M. D., Kutateladze, T. G. & Gozani, O. (2009). *Mol. Cell*, **33**, 248–256.
Iizuka, M., Sarmento, O. F., Sekiya, T., Scrable, H., Allis, C. D. & Smith, M. M. (2008). *Mol. Cell. Biol.* **28**, 140–153.
Kabsch, W. (1988). *J. Appl. Cryst.* **21**, 67–72.
Loewith, R., Meijer, M., Lees-Miller, S. P., Riabowol, K. & Young, D. (2000). *Mol. Cell. Biol.* **20**, 3807–3816.
Mellor, J. (2006). *Cell*, **126**, 22–24.
Palacios, A., Garcia, P., Padró, D., López-Hernández, E., Martín, I. & Blanco, F. J. (2006). *FEBS Lett.* **580**, 6903–6908.
Palacios, A., Moreno, A., Oliveira, B., Rivera, T., Prieto, J., García, P., Fernández-Fernández, M. R., Bernardó, P., Palmero, I. & Blanco, F. J. (2010). *J. Mol. Biol.* **396**, 1117–1127.
Palacios, A., Muñoz, I. G., Pantoja-Uceda, D., Marcaida, M. J., Torres, D., Martín-García, J. M., Luque, I., Montoya, G. & Blanco, F. J. (2008). *J. Biol. Chem.* **283**, 15956–15964.
Soliman, M. A. & Riabowol, K. (2007). *Trends Biochem. Sci.* **32**, 509–519.
Weiss, M. S. (2001). *J. Appl. Cryst.* **34**, 130–135.
Ythier, D., Larrieu, D., Brambilla, C., Brambilla, E. & Pedeux, R. (2008). *Int. J. Cancer*, **123**, 1483–1490.